

Hyperspherical partial wave theory applied to electron hydrogen-atom ionization calculation for equal energy sharing kinematics

J.N. Das and S. Paul

Department of Applied Mathematics, University College of Science, 92, Acharya Prafulla Chandra Road, Calcutta - 700 009, India

K. Chakrabarti

Department of Mathematics, Scottish Church College, 1 & 3 Uquhart Square, Calcutta - 700 006, India

Abstract

Hyperspherical partial wave theory has been applied here in a new way in the calculation of the triple differential cross sections for the ionization of hydrogen atoms by electron impact at low energies for various equal-energy-sharing kinematic conditions. The agreement of the cross section results with the absolute measurements of Roder et al [48] for different kinematic conditions at 17.6 eV is very encouraging. The other calculated results, for relatively higher energies, are also generally satisfactory, particularly for large angle geometries. In view of the present results, together with the fact that it is capable of describing unequal-energy-sharing kinematics [35], it may be said that the hyperspherical partial wave theory is quite appropriate for the description of ionization events of electron-hydrogen type systems. It is also clear that the present approach in the implementation of the hyperspherical partial wave theory is very appropriate.

PACS Nos 34.80.Dp, 34.50.Fa
e-mail: jndas@ucc.ernet.in

I. INTRODUCTION

In the study of electron hydrogen atom ionization collision, the simplest three-body ionization problem in atomic physics, there are many attempts for a complete solution but all of these face tremendous difficulties and have only limited success. Except for one or two attempts all use time-independent framework. For accurate information regarding scattering events, one may solve accurately the Schrödinger equation for the scattering states $|i\rangle^{(+)}_i$ or $|f\rangle^{(+)}_f$ [see Newton [1] for their definition] given by

$$H |i\rangle^{(+)}_{i,f} = E |i\rangle^{(+)}_{i,f} \quad (1)$$

taking account of the appropriate boundary conditions.

Ionization amplitudes may then be obtained either from the flux condition at infinity or from appropriate projections. In the literature both $|i\rangle^{(+)}_i$ and $|f\rangle^{(+)}_f$ have been widely used. There are a large number of attempts which strive to solve for $|i\rangle^{(+)}_i$. Among these the most successful attempts are the various close-coupling calculations [2-4]. In these calculations $|i\rangle^{(+)}_i$ are expanded in terms of basis functions and ionization information are extracted from a solution of the unknown expansion functions. Another possibility is to expand $|i\rangle^{(+)}_i$ in terms of a complete set of functions in the angular variables. In these regards the attempts of Kato and Watanabe [5, 6] are remarkable. They used hyperspherical co-ordinates and expanded $|i\rangle^{(+)}_i$ in terms of hyper-radius dependent angular functions. Matching with a wave function, which satisfies an approximately correct boundary condition, they obtained with remarkable success, the total ionization cross sections down to the threshold. However, differential cross section results of this theory are not known. Very recently Rescigno and associates made [7, 8] a breakthrough calculation and reproduced for equal energy-sharing and constant angular separation

of the outgoing electrons, the cross section results, at low energies, with surprising success. In these calculations they expanded $|i\rangle^{(+)}_i$ in terms of spherical harmonics in four angular variables. Then they converted the resultant differential equations for the radial functions, in two radial variables, into a set of difference equations over a large network in the radial variables plane. They used a novel technique. Using a complex scaling procedure they converted the scattering problem as if into a bound state problem. Then they solved a huge set (several million) of linear equations using very special techniques. Ultimately they obtained ionization amplitudes using the flux condition. Later [9] they confirmed their results using projection technique. Although the ECS approach reproduced the equal-energy-sharing, constant- ω results perfectly well, results of this approach for unequal-energy-sharing kinematics are not known. There are also large number of attempts of using $|f\rangle^{(+)}_f$ in extracting ionization information. In such cases projection approach has been generally used. There the ionization amplitudes are calculated from

$$T_{fi}^s = h |f\rangle^{(+)}_{fs} \langle j_{i,f} | \quad (2)$$

Brauner, Briggs and Klar [10] and later Berkdar [11] and Berkdar et al [12, 13] made use of this approach. They used $T_{fi}^{(1)}$ which are asymptotically correct (or nearly so) but are unlikely to be correct at finite distances. As a consequence results of these calculations are only moderately accurate. Moreover there are no systematic tractable way of improving the results.

An alternative approach for determining the electron atom collision cross sections is to solve a coupled set of integral equations for the on-shell T -matrix elements. Das and associates [14-16] have used this approach in the study of various electron hydrogen atom and electron helium atom scattering problems by solving the resultant equations in a rather crude manner. However, they always obtained moderately good results. There are also attempts [17-24] to improve the calculations. Among these lines the most successful calculations are the convergent close coupling (CCC) calculations of Bay et al [25-27]. In many contexts they applied the CCC method with surprising success. In the ionization calculations it is found to have several difficulties also [26, 28, 29].

Another promising approach for the electron hydrogen atom ionization problem is the hyperspherical partial wave approach [30-31]. Details of this approach are given in [31]. In section II we also present important features of this approach. Earlier with an additional approximation of neglecting the coupling effects, some results were obtained [32-33] which are qualitatively not very bad. Recently this approach has been used [34-35] retaining fully the coupling effects. In solving the relevant coupled set of radial wave equations over an initial interval $[0, R]$, R -matrix [36] approach had been used. Although the results were always found to be of the correct magnitude pseudo-resonance type behaviour gives much troubles in extracting correct cross section results. To avoid this problem we use a new approach. This appears to be very successful and leads to very interesting results both for equal-energy-sharing constant- ab kinematics, equal-energy-sharing asymmetric kinematics, and also for unequal-energy-sharing kinematics [35]. Thus it appears that hyperspherical partial wave theory is quite appropriate for the study of ionization problems of electron-hydrogen type systems.

Most recently two very broad-based theories have been proposed. One of these is the time-dependent close coupling theory [37] and the other is the hyperspherical R -matrix theory [38]. Positions of these theories are not yet very clear.

II. HYPERSPHERICAL PARTIAL WAVE THEORY

In the hyperspherical partial wave theory one uses the time-independent framework. In the time-independent framework the T -matrix element is given by expression (2) or alternatively by

$$T_{fi} = h_f \mathcal{Y}_f j_i^{(+)} i: \quad (3)$$

In these expressions i and f are the unperturbed initial and final channel wave functions, satisfying certain exact boundary condition at infinity and that the V_i and V_f

are the corresponding perturbation potentials. For the case of ionization of hydrogen atom's expression (2) is more appropriate for use, since in this case asymptotically correct ψ is easily available. Many use expression (3), including ECS [9] by projection method, but inappropriately, since the corresponding ψ_f 's they use do not satisfy the correct boundary condition. In the hyperspherical partial wave theory ψ_f is expanded in terms of hyperspherical harmonics, which are functions of five angular variables. The corresponding radial waves are functions of one radial variable, the hyper radius R only. This proves to be advantageous in numerical computations, since then the five angular variables range over a bounded compact domain, while only one variable R ranges over a semi-infinite domain $[0; \infty)$. It may be noted here that so far nobody could take account of the exact boundary condition in the asymptotic domain for the accurate solution of ψ_f . Here we aspire to take account the exact boundary condition at infinity, in the limit. This is the most novel feature in the hyperspherical partial wave theory. Here we may note that two plane waves $\exp(ip_a \cdot \mathbf{r} + ip_b \cdot \mathbf{r}) = (2)^{3/2}$ and $\exp(ip_b \cdot \mathbf{r}) = (2)^{3/2}$ may be decomposed in partial waves as usual and then these may be combined (using a formula in Erdelyi [39]) to obtain an expansion in terms of hyperspherical harmonics (!), in five angular variables $\psi = (\psi_0; \psi_1; \psi_2; \psi_3; \psi_4)$. A symmetrized two-particle plane wave has the expansion [Das, 31]

$$\begin{aligned} & \exp(ip_a \cdot \mathbf{r} + ip_b \cdot \mathbf{r}) + (-1)^s \exp(ip_b \cdot \mathbf{r} + ip_a \cdot \mathbf{r}) = (2)^3 \\ & = 2 \cdot \frac{1}{2} \cdot X \cdot i \cdot \frac{j(\psi)}{\frac{3}{2}} \cdot s(\psi_0) \cdot s(\psi_1); \end{aligned} \quad (4)$$

where $\psi = \psi_0 + \frac{3}{2}$ and $\psi = \frac{1}{2}(\psi_1 + \psi_2 + 2\psi_3)$ (ψ also denotes the multiplet $(l_1; l_2; n)$ depending on the context). Here $R = \sqrt{r_1^2 + r_2^2}$, $\psi_0 = \text{atan}(r_2 = r_1)$, $r_1 = (r_1; \psi_1; \psi_0)$, $r_2 = (r_2; \psi_2; \psi_0)$. Similarly $P = p_a^2 + p_b^2$, $\psi_0 = \text{atan}(p_b = p_a)$, $p_a = (p_a; \psi_a; \psi_a)$, $p_b = (p_b; \psi_b; \psi_b)$, and $\psi = PR$, and $\psi_0 = (\psi_0; \psi_a; \psi_a; \psi_b; \psi_b)$,

$$\begin{aligned} s(\psi) &= \frac{1}{2} f P_{l_1 l_2}^n(\psi) Y_{l_1 l_2}^{LM}(\hat{r}_1; \hat{r}_2) + (-1)^{l_1 + l_2 - L + S + n} P_{l_2 l_1}^n(\psi) Y_{l_2 l_1}^{LM}(\hat{r}_1; \hat{r}_2) g; l_1 \neq l_2 \\ &= \frac{1}{2} f \psi_1 + (-1)^{L + S + n} g P_{l_1 l_1}^n(\psi) Y_{l_1 l_1}^{LM}(\hat{r}_1; \hat{r}_2) g; \text{ for } l_1 = l_2 = l; \end{aligned} \quad (5)$$

and a corresponding expression for $s(\psi_0)$ (Similar expressions may be easily derived for product of more than two plane waves).

Now the symmetrized wave ψ_{fs} may be expanded in terms of symmetrized hyperspherical harmonics s 's as

$$\psi_{fs}(R; \psi) = 2 \cdot \frac{1}{2} \cdot X \cdot \frac{F^s(\psi)}{\frac{5}{2}} \cdot s(\psi_0); \quad (6)$$

where F^s satisfy an infinite coupled set of equations

$$h \frac{d^2}{dR^2} + P^2 - \frac{(\psi + 1)^2}{R^2} F^{(s)}(R) + \frac{X}{R} \frac{2P}{R} F_0^{(s)}(R) = 0; \quad (7)$$

for each symmetry s ($s = 0$ for singlet and $s = 1$ for triplet) and for each total angular momentum L (and its projection M , and so also for a definite parity). In the above expression

$$s_0 = h^s \mathbf{C} j^s \mathbf{i} = \mathbf{P}; \text{ and}$$

$$C = \frac{1}{\cos} - \frac{1}{\sin} + \frac{1}{j_1 \cos - j_2 \sin}:$$

The equations (7) have to be solved over the semi-infinite domain $[0; 1]$. Solution in the asymptotic domain is simple. The equations have nice asymptotic solutions. One may note that because of conservation rules the equations (7) are decoupled into sets for fixed $= (L; S;)$ and different $N = (l_1; l_2; n)$. So we set $F^{(s)} = f_N$ and, for the set with fixed (and dropping from f_N) we can write equations (7) as

$$\frac{h}{dR^2} + P^2 - \frac{N(N+1)}{R^2} f_N^i + \frac{X}{N^0} \frac{2P}{R} f_N^0 = 0; \quad (8)$$

for a solution over the finite domain and

$$\frac{h}{d^2} + 1 - \frac{N(N+1)}{2} f_N^i + \frac{X}{N^0} \frac{2}{R} f_N^0 = 0; \quad (9)$$

for solution over an asymptotic domain, say $[R_0; 1]$. Next we consider the solution problem first over an asymptotic domain $[R_0; 1]$ and then over the finite domain $[0; R_0]$.

A. Solution in an asymptotic domain

The equations (9) have two sets of solutions [31] in an asymptotic domain $[R_0; 1]$ of the form given by

$$f_{snN}^{(k)}() = \begin{cases} \frac{x}{\omega_0} \frac{a_{kn}^{(1)} \sin \omega_k}{\omega_0} + \frac{x}{\omega_0} \frac{b_{kn}^{(1)} \cos \omega_k}{\omega_0}; \\ \omega_0 \end{cases} \quad (10)$$

$$f_{csN}^{(k)}() = \begin{cases} \frac{x}{\omega_0} \frac{c_{kn}^{(1)} \sin \omega_k}{\omega_0} + \frac{x}{\omega_0} \frac{d_{kn}^{(1)} \cos \omega_k}{\omega_0}; \\ \omega_0 \end{cases} \quad (11)$$

where $\omega_k = + \omega_k \ln 2$ and ω_k is the k -th eigen value of the charge matrix $A = (a_{nn})$ and that the coefficients $a_{kn}^{(1)}$; $b_{kn}^{(1)}$; $c_{kn}^{(1)}$ and $d_{kn}^{(1)}$ are determined from recurrence relations. Thus the coefficients $a_{kn}^{(1)}$ and $b_{kn}^{(1)}$ are determined from the relations -

$$2[(A_k)^2 + l^2 I]X_k^{(1)} = A_{k-k} - l(l-1)A_k - l(2l-1)_{-k} I X_k^{(1-1)} \\ + [(2l-1)_{-k} A_k + l_{-k} - l^2(l-1)I]Y_k^{(1-1)} \quad (12)$$

and

$$2[(A_k)^2 + l^2 I]Y_k^{(1)} = A_{k-k} - l(l-1)A_k - l(2l-1)_{-k} I Y_k^{(1-1)} \\ + [(2l-1)_{-k} A_k + l_{-k} - l^2(l-1)I]X_k^{(1-1)} \quad (13)$$

where the N -th components of vectors $X_k^{(1)}$ and $Y_k^{(1)}$ are given by

$$(X_k^{(1)})_N = a_{kN}^{(1)}; (Y_k^{(1)})_N = b_{kN}^{(1)}$$

and where

$$A_k = A - kI; (A_k)_{NN^0} = [k^2 + N(N+1)]_{NN^0}$$

The initial vectors $X_k^{(0)}$ and $Y_k^{(0)}$ are given by

$$X_k^{(0)} = X_k; Y_k^{(0)} = 0;$$

X_k being the k -th eigen vector of the charge matrix A and I is the identity matrix. Solution for $c_{kN}^{(1)}$'s and $d_{kN}^{(1)}$'s are similarly obtained from the above recurrence relations after setting $X_k^{(0)} = 0$ and $Y_k^{(0)} = X_k$. In this way we get solution vectors $f_{snN}^{(k)}$ and $f_{csN}^{(k)}$ of equations (10) and (11).

B . Solution over a nite domain

Here we consider the solution of equations (8) over a nite domain $[0; R_0]$. Away from the origin, solution of the equations is easy. A Taylors series expansion method succeeds for getting arbitrarily accurate solutions. The main difficulty is in starting the solution from the origin. Near origin the equations have analytic solutions (Fock [40]) but these are too complicated to be useful in numerical computations. In our earlier calculations [34-35] we used R-matrix approach for getting solutions over an initial interval $[0;]$ (with $]$ suitably chosen). But this approach faces troubles as pseudo-resonance type behavior appears giving much troubles in determining appropriate solutions. To avoid such difficulties we consider here a new approach. For the interval $[0;]$ we consider a boundary value problem. The solution vector $f_0^{(k)}(R)$ is assumed to have a value 0 at the origin and the k -th column of the $N_{m \times} N_{m \times}$ identity matrix at $R = 0$. We divide the interval $[0;]$ into m subintervals and use a ve-point difference formula

$$f_N^{(0)}(R_k) = \frac{1}{12h^2} [f_N(R_{k-2}) + 16f_N(R_{k-1}) - 30f_N(R_k) + 16f_N(R_{k+1}) - f_N(R_{k+2})] + \frac{h^4}{90} f_N^{(vi)}()g \quad (14)$$

for $k = 2; 3; \dots; m-2$, and a formula

$$f_N^{(0)}(R + h^0) = 2f_N^{(0)}(R + 2h^0) - f_N^{(0)}(R + 3h^0) + \frac{1}{h^2} [f_N(R) - 4f_N(R + h^0) + 6f_N(R + 2h^0) - 4f_N(R + 3h^0) + f_N(R + 4h^0)] + f \frac{h^4}{12} f_N^{(vi)}()g; \quad (15)$$

with $R = R_0, h^0 = h$ for the equation at $R = R_1$ and $R = R_m, h^0 = h$ for the equation at $R = R_{m-1}$. For continuing solutions from onward we need first order derivatives at

. For this we use the simple formula

$$\begin{aligned} f_N^0(R_m) &= [f_N(R_{m-4}) + 24f_N(R_{m-2}) - 128f_N(R_{m-1}) + 105f_N(R_m)] = (84h) \\ &+ \frac{2h}{7}f_N^\infty(R_m) + f \frac{4h^4}{105}f_N^{(v)}()g: \end{aligned} \quad (16)$$

The resultant linear set of equations ultimately take the form

$$S Y^{(k)} = b; \quad (17)$$

where S is a sparse matrix. We solve these equations by the biconjugate gradient method [41] using routines given in [42]. With a suitable choice of a preconditioner the iterations smoothly converge (with a few hundred iterations or even less) to five or six decimal places for a suitable choice of error limit (say, 1 in 10^7 parts). In this way N_{m_x} solution vectors $f_0^{(k)}$ are determined over $[0; R_0]$. The solutions are next continued over $[; R_0]$ by Taylors expansion method with stabilisation [43] after suitable steps, giving solution vectors $f_0^{(k)}$ over $[0; R_0]$.

C. Matching of the solutions: Determination of $f_{fs}^{(k)}$

For finding the physical solution vectors f_{ph} and the scattering state $f_{fs}^{(k)}$ we first define solution matrices f_0 , f_{sn} and f_{cs} , by putting side by side the corresponding solution vectors $f_0^{(k)}$, $f_{sn}^{(k)}$, $f_{cs}^{(k)}$, for $k = 1; 2; \dots; N$. Then the physical solution vector f_{ph} may be defined over $[0; R_0]$ by

$$f_{ph}(R) = \sum_{k=1}^{N_{m_x}} g_k f_0^{(k)}(R) \quad (18)$$

and over $[R_0; 1]$ by

$$f_{ph}(R) = \sum_{k=1}^{N_{m_x}} c_k f_{sn}^{(k)}() + \sum_{k=1}^{N_{m_x}} d_k f_{cs}^{(k)}(): \quad (19)$$

$2N_{m_x}$ of the $3N_{m_x}$ unknown coefficients are now determined by matching values (and first order derivatives) of the two sets of solutions at a point R_0 where all the solutions are valid. The remaining N_{m_x} unknown coefficients are then determined from the demand that $f_{fs}^{(k)}$ actually satisfies the appropriate boundary condition. To facilitate the computations we first define the K -matrix through the relation

$$f_0 B = f_{sn} + f_{cs} - K \quad (20)$$

where B is some unknown constant matrix. (The K -matrix thus defined is a little different from the one usually defined. But in any case it should be symmetric.). The K -matrix

is then determined by matching values and first order derivatives of the two sides of equation (20). Then in the asymptotic domain one has

$$\begin{aligned} f_{ph} &= (f_{sn} + f_{cs} - K) \cdot c \\ &= f_{sn} \cdot c + f_{cs} \cdot d; \end{aligned} \quad (21)$$

where

$$d = K - c; \quad (22)$$

Finally f_{ph} is completely determined once the vector c is determined. Now c is determined from the consideration that $\left| f_s \right\rangle$ is asymptotically a distorted plane wave (representing the two outgoing electrons) plus incoming waves only. So we equate coefficients of the outgoing wave $\exp(i \cdot \vec{p}_s)$ of both $\left| f_s \right\rangle$ and the symmetrized plane wave (4) (except for the distorting term $s \exp(i \cdot \vec{k} \ln 2)$). This gives

$$c = \frac{h}{I + iK} \cdot \frac{i}{P} \quad (23)$$

where

$$P = e^{\frac{i}{4} X^{-1}} \cdot (s) \cdot (1_0);$$

where X is the matrix consisting of eigen vectors of the charge matrix A (and is non-singular) and $(s) \cdot (1_0)$ is given by

$$s \cdot (1_0) = \begin{bmatrix} 0 & & & 1 \\ & s_1 \cdot (1_0) & & \\ B & & C & \\ @ & \vdots & A & \\ & & s_{N_m x} \cdot (1_0) & \end{bmatrix} \quad (24)$$

In this way the physical radial vectors $f_{ph}(R)$ are determined for each $= (L; S; \cdot)$ and ultimately the full (but approximate) scattering state $\left| f_s \right\rangle$ is obtained.

Substituting this expression in equation (2) one obtains the scattering amplitude in the form

$$f^s(1_0) = \frac{1}{2} T_{fi}^s = \frac{1}{2} \frac{X}{N} \cdot C^s(N) \cdot \frac{s}{N} \cdot (1_0) \quad (25)$$

The triple differential cross section is then given by

$$\frac{d^3}{dE_{ad} da d_b} = \frac{(2)^4 p_a p_b}{p_i} \frac{N}{4} \left(\frac{1}{4} \mathcal{T}_{fi}^{(0)} \hat{f} + \frac{3}{4} \mathcal{T}_{fi}^{(1)} \hat{f} \right)^{\circ} \quad (26)$$

By increasing the number of channels $N_{m x}$ for each $= (L; S; \cdot)$ one may expect to obtain converged cross section results.

III. PRESENT CALCULATION

In our present calculation for the equal-energy-sharing constant - $_{ab}$ kinematic conditions, where $_{ab}$ is the angular separation of the outgoing electrons, there are two important parameters α and R_0 which are needed to be judiciously chosen. The parameters

of the initial interval $[0, 1]$, for a solution of the radial equations (8), has been chosen to be 5 a.u. for all the energies considered here. The results do not depend on R_0 for small variations (of a few a.u.) about this value. On the other hand the choice of the parameter R_0 , the asymptotic range parameter, is very crucial. Without its appropriate choice the asymptotic series solutions (10) and (11) are unlikely to converge. Here it is found that for convergent asymptotic series solutions R_0 is needed to be such that $R_0 = \frac{1}{E}$, where E is the energy in the final channel. Thus for energies of 30 eV, 25 eV, 19.6 eV, 17.6 eV, and 15.6 eV this range parameter R_0 may be chosen greater than the values 60 a.u., 70 a.u., 90 a.u., 120 a.u. and 150 a.u. respectively. We have chosen R_0 around these values in our calculations. However for the computation of single differential cross section (SDCS) it is necessary for converged results to vary R_0 , and extrapolate, as in ECS calculation [8] for R_0 ! Our limited computational resources restrict us to take single R_0 value for each energy. Moreover for arbitrary large R_0 unwanted errors are likely to make the results erroneous. So some optimum choice of R_0 has to be made for each energy with a few trials. In our present computations this has been done. Next we consider the choice of L values for inclusion in the calculations for different energies. For 15.6 eV energy, values of L upto 5 proved sufficient. For 17.6 eV calculations values of L upto 7 are found to be necessary. For the other energies, considered here, values of L upto 9 have been included. For fixed $(L; S; \lambda)$ the number of channels, the number of states with different (l_1, l_2, n) triplets, which have been included, were chosen suitably for fairly converged results. In any case for fixed (l_1, l_2) pairs n was varied from 0 to 9. In this way convergence with respect to n is obtained. The number of (l_1, l_2) pairs, which have been included, are somewhat less for $L = 2$ compared to those in the ECS calculation. These pairs are chosen more or less in the order as in ECS calculations (a little different from those of hyperspherical calculations of Kato and Watanabe [6]). However there could be some better choice. For lower energies convergence with respect to the increase in channel size is rather smooth. It is not so for relatively higher energies of 25 eV or 30 eV. Nevertheless we have obtained nearly converged results in the cases considered. All the results presented here are more or less based on 50 channels calculations. Most of the calculations, reported here, were done on Pentium-III PCs. Calculations for 15.6 eV energy could not be done on PCs. Thus the results for 15.6 eV and 17.6 eV, which are presented here, have been derived from calculations on a SUN server. It may be further added here that for 15.6 eV the SDCS results show that for equal energy sharing case the calculated SDCS value is about twice the expected value, although the calculated total cross section appears correct (see table I). This is unacceptable. In any case the various cross section results for this energy have been multiplied by a factor 0.5 before presentation in the figures. For other energies, however, we have nearly the correct SDCS values for equal energy sharing situations. Calculation on a larger scale with larger values of R_0 , and with more precise solution of the equations (17), may decide absolutely the normalization question of the measured results of Roder et al [45] for 15.6

eV energy. Cross section results for 15.6 eV energy have been included here for the sake of completeness.

IV . R E S U L T S

A . Triple Differential Cross Section for Constant $_{ab}$ Geometry

The triple differential cross section results for equal-energy-sharing constant $_{ab}$ geometries are presented in figures 1 (a) for 15.6 eV energy, in figure 2 (a) for 17.6 eV energy and in figures 3,4 and 5 for energies of 19.6 eV, 25 eV and 30 eV. In these figures we have presented the theoretical results of CCC calculations [26,46] and of ECS calculations [8,47]. Here we have also included the absolute measured values of Roder et al[44,45] for 15.6 eV and the most recent remeasured (with necessary inter-normalization) values of Roder et al[48] for 17.6 eV energy. For other energies the measured results [44] are only relative and are normalized as in [9]. Our results are generally comparable with the ECS results in magnitude. For 17.6 eV our present results appear most interesting. These are even somewhat better compared to the ECS results for $_{ab} = 150^\circ$ and 180° . For these values of $_{ab}$, the 15.6 eV results also appear good, particularly in shapes, but confirmation by larger scale calculation is necessary. The 19.6 eV results also appear to be very good. For other energies our results appear less satisfactory in comparison with the ECS results, but are generally comparable with the CCC results.

B . Triple Differential Cross Sections for Fixed $_{a}$ Geometry

In figures 1 (b) and 2 (b) we have compared our results for equal-energy-sharing asymmetric geometries with absolute measured values of Roder et al[45] for 15.6 eV and Roder et al[48] for 17.6 eV, in which one of the outgoing electrons is observed in a fixed direction while that of the other one is varied. In these cases we again compare our results with the calculated results of ECS and CCC theories. Here our results also appear to be quite good, particularly for 17.6 eV in view of the most recent measurements. For $_{a} = 30^\circ$ at 15.6 eV, the peak position of our calculated curves are little shifted to the right. Otherwise all the results of the present calculation appear satisfactory.

C . Triple Differential Cross Sections for Symmetric Geometry

In figures 1 (c) and 2 (c) we have presented TDCS results for symmetric appearance of the two outgoing electrons relative to the incident electron direction, for 15.6 eV and 17.6 eV incident electron energies, for which there are again absolute measured results [45,48]. For 15.6 eV energy our results agree qualitatively with the experimental results. Here a 70-channel calculation has been found to be necessary. For 17.6 eV our results do not appear very good. For 15.6 eV energy both the ECS and CCC theories underestimate

the cross section results considerably. For 17.6 eV energy, however, the ECS theory gives the best overall representation.

D . Integrated Cross Sections and the Spin Asymmetry Parameter
 The parabolic fitted curves to our computed single differential cross sections data are generally close to the ECS extrapolated curves but our raw data which could be calculated, as in ECS flux method, only away from the two ends of the energy intervals widely differ from ECS or CCC (wherever available) curves. However, the computed total integrated cross sections, with suitable extrapolation from these are generally good. Here in table I we have presented values of integrated cross sections $I = (s + 3t)/4$ and the spin asymmetry parameter $A = (s - t)/(s + 3t)$ where s and t are the singlet and the triplet cross sections, together with values of ECS theory by flux approach [8] and those of CCC theory and the experimental values. The integrated cross sections agree with the experimentally measured values of Shah et al[49] within about 20%. The spin asymmetry parameter A agrees, however, excellently with the measurements [50,51].

Next we note down the shortcomings and difficulties associated with the present approach. The first point to note is that it may not be possible in this approach to get reliable cross section results for extreme asymmetry, as in ECS flux approach, for one of the outgoing electrons sharing very small energy values compared to the other. 'Contamination with high Rydberg states', as in ECS calculation [8] gives wrong results for finite values of R_0 in such cases. Extrapolation to $R_0 = 1$ may only lead to reliable results in those cases. This may require larger computational resources. Another difficulty to be noted is the appearance of a few large eigen-values of the charge matrix for large-channel calculations. In such cases computational strategies are needed to be reviewed. In our calculations this has occurred in a few cases. In such cases we simply cut-short in magnitude these one or two large eigen values to the neighboring ones. However a better approach may be necessary to tackle such problems. No other difficulties appear worth mentioning. For a fully converged results inclusion of more channels (about 100 or a little more) may be required with appropriate choice of $(l_1; l_2)$ pairs (say, as in ECS calculation) and with further stabilization. However these are subjects of further studies requiring more computational resources and time.

V . CONCLUSIONS

The results of the present calculation fairly display the capability of the hyperspherical partial wave theory in representing results for equal-energy-sharing kinematical conditions at low energies. The new approach that has been used in the implementation of the hyperspherical partial wave theory appears very appropriate. The computed cross section results are observed to be very satisfactory. If one recalls the capability of the theory to

describe the ionization collisions for unequal-energy-sharing asymmetric kinematic conditions (as indicated in [35]) also then the capability of the hyperspherical partial wave theory towards a complete description of the electron -hydrogen -atom ionization problem is amply demonstrated. Considering the computational facilities used (Pentium - III PCs and a SUN Enterprise 450 server) success of the present calculation is appreciable. For fully converged results better computational facilities may be required. The theory may easily be applied in the study of ionization of hydrogen-like ions with a little change in the definition of the wave function ψ_i and the interaction potential V_i . The theory may also be extended for application to the double-ionization of helium atom or helium-like ions or to other multi-electron ionization processes.

V I. ACKNOWLEDGMENTS

The authors are grateful to Igor Bray for providing with the CCC results and the experimental results of Roder et al in electronic form. They are also grateful to T.N. Rescigno and M. Baertschy for sending the ECS results electronically. Special thanks are also due to M. Baertschy for providing Matlab scripts which helped in drawing the figures. S. Paul is grateful to CSIR for providing a research fellowship.

References

- [1] R . G . Newton, *Scattering Theory of Waves and Particles*, McGraw-Hill, NY (1966).
- [2] E . P . Curran and H . R . J . W alters, *J . Phys . B* 20, 337 (1987); see also E . P . Curran, C . T . W helan and H . R . J . W alters, *J . Phys . B* 24, L19 (1991).
- [3] K . Bartchat, E . T . Hudson, M . P . Scott, P . G . Burke, and V . M . Burke, *J . Phys . B* 29, 115 (1996).
- [4] K . Bartschat and I . Bray, *J . Phys . B* 29, L577 (1996).
- [5] D . Kato and S . W atanabe, *Phys . Rev . Lett* 74, 2443 (1995).
- [6] D . Kato and S . W atanabe, *Phys . Rev A* 56, 3687 (1997).
- [7] T . N . Rescigno, M . Baertschy, W . A . Isaacs, and C . W . M cCurdy, *Science* 286, 2474 (1999).
- [8] M . Baertschy, T . N . Rescigno, W . A . Isaacs, X . Li, and C . W . M cCurdy, *Phys . Rev . A* 63, 022712 (2001).
- [9] M . Baertschy, T . N . Rescigno, and C . W . M cCurdy, *Phys . Rev . A* 64, 022709 (2001).
- [10] M . Brauner, J . S . Briggs, and H . Klar, *J . Phys . B* 22, 2265 (1989).
- [11] J . Berakdar, *Phys . Rev . A* 53, 2314 (1996).
- [12] J . Berakdar, J . Roder, J . S . Briggs, and H . Ehrhardt, *J . Phys . B* 29, 6203 (1996).
- [13] J . Berakdar, J . S . Briggs, I . Bray, and D . V . Fursa, *J . Phys . B* 32, 895 (1999).
- [14] J . N . Das, *J . Phys . B* 11, L195 (1978).
- [15] J . N . Das, *Phys . Lett A* 69, 405 (1979); *ibid* 83, 428 (1981).
- [16] J . N . Das, R . K . Bera, and B . Patra, *Phys . Rev . A* 23, 732 (1981).
- [17] J . N . Das and A . K . Biswas, *Phys . Lett A* 78, 319 (1980).
- [18] J . N . Das and A . K . Biswas, *J . Phys . B* 14, 1363 (1981).
- [19] J . N . Das and P . K . Bhattacharyya, *Phys . Rev . A* 27, 2876 (1983).
- [20] J . N . Das and N . Saha, *J . Phys . B* 14, 2657 (1981).
- [21] J . N . Das and N . Saha, *Pramana-J . Phys .* 18, 397 (1982).
- [22] J . N . Das, A . K . Biswas, and N . Saha, *Aust . J . Phys .* 35, 393 (1982).
- [23] J . N . Das and A . K . Biswas, *Czech . J . Phys . B* 38, 1140 (1988).
- [24] S . P . K hare and K usum Lata *Phys . Rev . A* 29, 3137 (1984); S . P . K hare and Satya Prakash, *Phys . Rev . A* 32, 2689 (1985).
- [25] I . Bray, D . A . K onovalov, I . E . M cCarthy, and A . T . Stelbovics, *Phys . Rev . A* 50, R2818 (1994).
- [26] I . Bray, *J . Phys . B* 32, L119 (1999); *J . Phys . B* 33, 581 (2000).
- [27] I . Bray, *Aust . J . Phys .* 53, 355 (2000).
- [28] G . Bencze and C . C handler, *Phys . Rev . A* 59, 3129 (1999).
- [29] S . Jones and D . H . M adison, *Phys . Rev . A* 63, 042701 (2000).
- [30] J . N . Das, *Aust . J . Phys .* 47, 743 (1994).
- [31] J . N . Das, *Pramana-J . Phys .* 50, 53 (1998).
- [32] J . N . Das and K . Chakrabarti, *Pramana-J . Phys .* 47, 249 (1996).

[33] J. N. Das and K. Chakrabarti, *Phys. Rev. A* **56**, 365 (1997).

[34] J. N. Das, *Phys. Rev. A* **64**, 054703 (2001).

[35] J. N. Das, *J. Phys. B* **35**, 1165 (2002).

[36] P. G. Burke and W. D. Robb, *Adv. At. Mol. Phys.* **11**, 143 (1975).

[37] M. S. Pindzola and F. Robicheaux, *Phys. Rev. A* **55**, 4617 (1997); *ibid* **57**, 318 (1998); *ibid* **61**, 052707 (2000).

[38] L. M. alegrat, P. Selles, and A. K. azansky, *Phys. Rev. A* **60**, 3667 (1999).

[39] A. Erdelyi, *Higher Transcendental Functions*, Vol II, p.99. McGraw-Hill, NY (1953).

[40] V. Fock, *K. Norske Vidensk. Selsksh. Forh* **31**, 138 (1958).

[41] R. Fletcher, *Numerical Analysis Dundee*, 1975, Lecture Notes in Mathematics, Vol. 506, Eds. A. Dold and B. Eckmann, Springer-Verlag, Berlin, pp 73-89 (1976).

[42] W. H. Press, S. A. Teukolsky, W. T. Vetterling, and B. P. Flannery, *Numerical Recipes in Fortran*, p77, 2nd ed., Cambridge University Press (1992).

[43] B. H. Choi and K. T. Tang, *J. Chem. Phys.* **63**, 1775 (1975).

[44] J. Roder, J. Rasch, K. Jung, C. T. W. helan, H. Ehrhardt, R. J. Allan, H. R. J. Walters, *Phys. Rev. A* **53**, 225 (1996).

[45] J. Roder, H. Ehrhardt, C. Pan, A. F. Starace, I. Bray, and D. Fursa, *Phys. Rev. Lett.* **79**, 1666 (1997).

[46] I. Bray, private communications.

[47] M. Baertschy and T. N. Rescigno, private communications.

[48] J. Roder, M. Baertschy and I. Bray, *Phys. Rev A* **45**, 2951 (2002) (to be published).

[49] M. B. Shah, D. S. Elliot, and H. B. G. ilbody, *J. Phys. B* **20**, 3501 (1987).

[50] D. M. Crowe, X. Q. Guo, M. S. Lubell, J. Slevin, and M. Emeryan, *J. Phys. B* **23**, L325 (1987).

[51] G. D. Fletcher, M. J. Agar, T. J. Gray, P. F. Wainwright, M. S. Lubell, W. Raith and V. W. Hughes, *Phys. Rev. A* **31**, 2854 (1985).

TABLE

Table I. Total integrated ionization cross sections (a.u.) and the spin asymmetry parameter. The experimental values of cross sections are those of Shah et al [49] (the starred numbers are from extrapolation). ECS results are from [8] and the CCC results are from [4]. In the experimental results of the asymmetry parameter of Crowe et al [50] and Fletcher et al [51] presented here, the numbers with superscript + or - denote the available result just a little above or below the energy considered (for the exact energy values the corresponding references are to be seen). For 15.6 eV energy, ECS results of earlier calculation [8] are not available. So for this energy we present results from [9] and indicate it so in the table.

E_i (eV)	30	25	19.6	17.6	15.6
Total Integrated Cross Sections					
Present:	2.13	1.82	1.14	0.83	0.49
ECS:	1.79	1.62	1.09	0.80	0.36 [9]
CCC:	1.92	1.57	1.01	0.75	0.38
Expt.:	1.81	1.55	1.00	0.74	0.39
Spin Asymmetry					
Present:	0.31	0.41	0.47	0.55	0.48
ECS:	0.42	0.45	0.51	0.51	0.52 [9]
CCC:	0.41	0.43	0.50	0.51	0.53
Expt.:					
Crowe	0.28	0.39	0.42	0.47	0.50
Fletcher	0.31	0.41	0.40 ⁺	0.50	0.48

Figure C options

Figure 1 (a). TDCS in coplanar equal-energy-sharing constant angular separation α of the outgoing electrons for incident electron energy $E_i = 15.6$ eV vs. ejection angle α of the slow outgoing electron. Continuous curves, present results; dashed-curves, ECS results [9,47]; dash-dotted curves, CCC results [26,46]. The experimental results are the absolute measured values of Roder et al [45,46]. Present results have been multiplied by a factor 0.5 (see text).

Figure 1 (b). TDCS in coplanar equal-energy-sharing geometry for incident electron energy $E_i = 15.6$ eV for fixed α and variable β of the outgoing electrons. Continuous curves, present results; dashed-curves, ECS results [9,47]; dash-dotted curves, CCC results [26,46]. The experimental results are the absolute measured values of Roder et al [45,46]. Present results have been multiplied by a factor 0.5 (see text).

Figure 1 (c). TDCS in coplanar equal-energy-sharing with two electrons emerging on opposite sides of the direction of the incident electron with equal angle α and energy $E_i = 15.6$ eV. Continuous curves, present results; dashed-curves, ECS results [9,47]; dash-dotted curves, CCC results [26,46]. The experimental results are the absolute measured values of Roder et al [45,46]. Present results have been multiplied by a factor 0.5 (see text).

Figure 2 (a). Same as in figure 1(a) but for 17.6 eV incident electron energy and the experimental results are the recent absolute measured values of Roder et al [48]. Here the present results are free from any multiplicative factor.

Figure 2 (b). Same as in figure 1(b) but for 17.6 eV incident electron energy and the experimental results are the recent absolute measured values of Roder et al [48]. Here the present results are free from any multiplicative factor.

Figure 2 (c). Same as in figure 1(c) but for 17.6 eV incident electron energy and the experimental results are the recent absolute measured values of Roder et al [48]. Here the present results are free from any multiplicative factor.

Figure 3. Same as in figure 2(a) but for 19.6 eV incident electron energy. The relative measured results of Roder et al [44-46] are normalized as in [9].

Figure 4. Same as in figure 3 but for 25 eV incident electron energy.

Figure 5. Same as in figure 3 but for 30 eV incident electron energy.

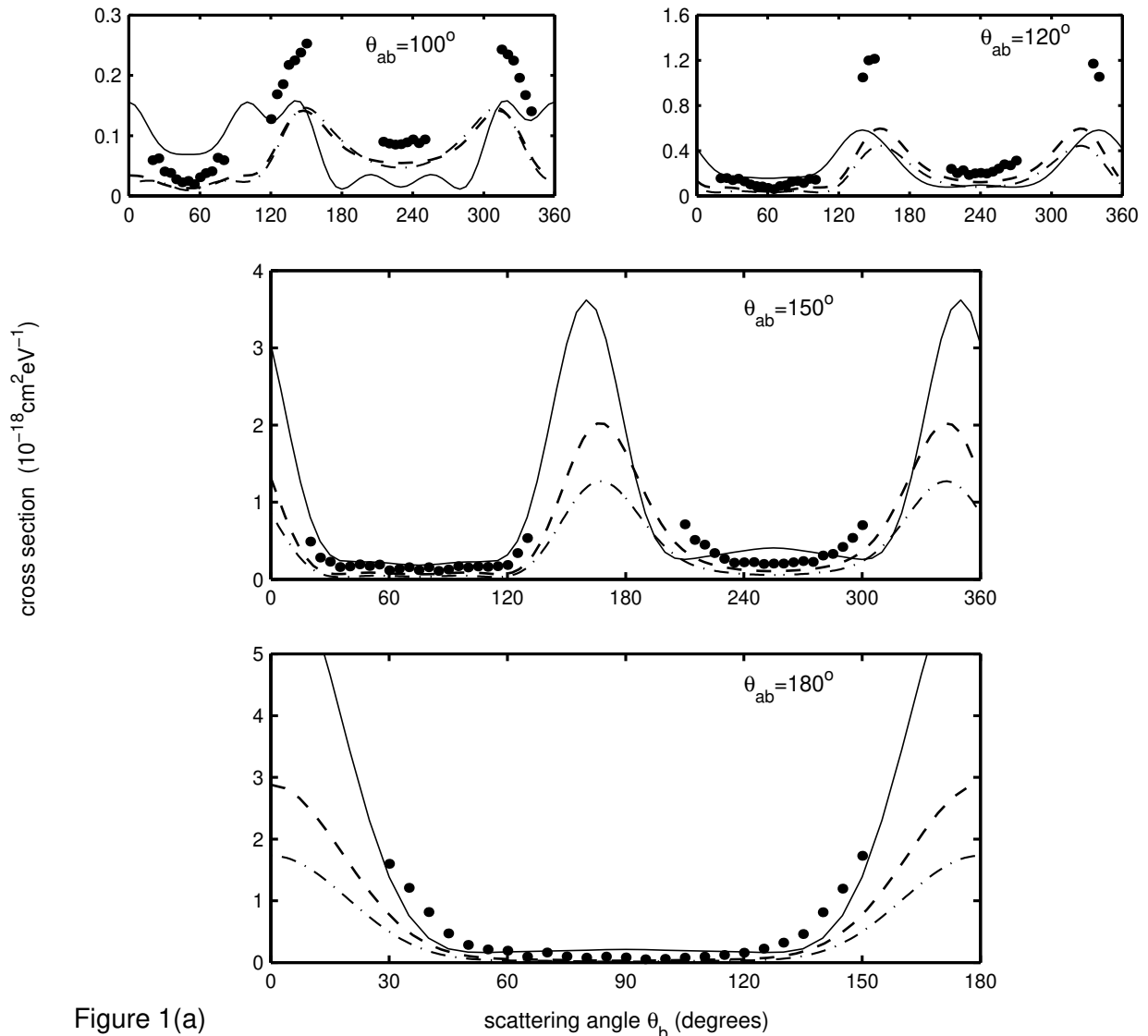


Figure 1(a)

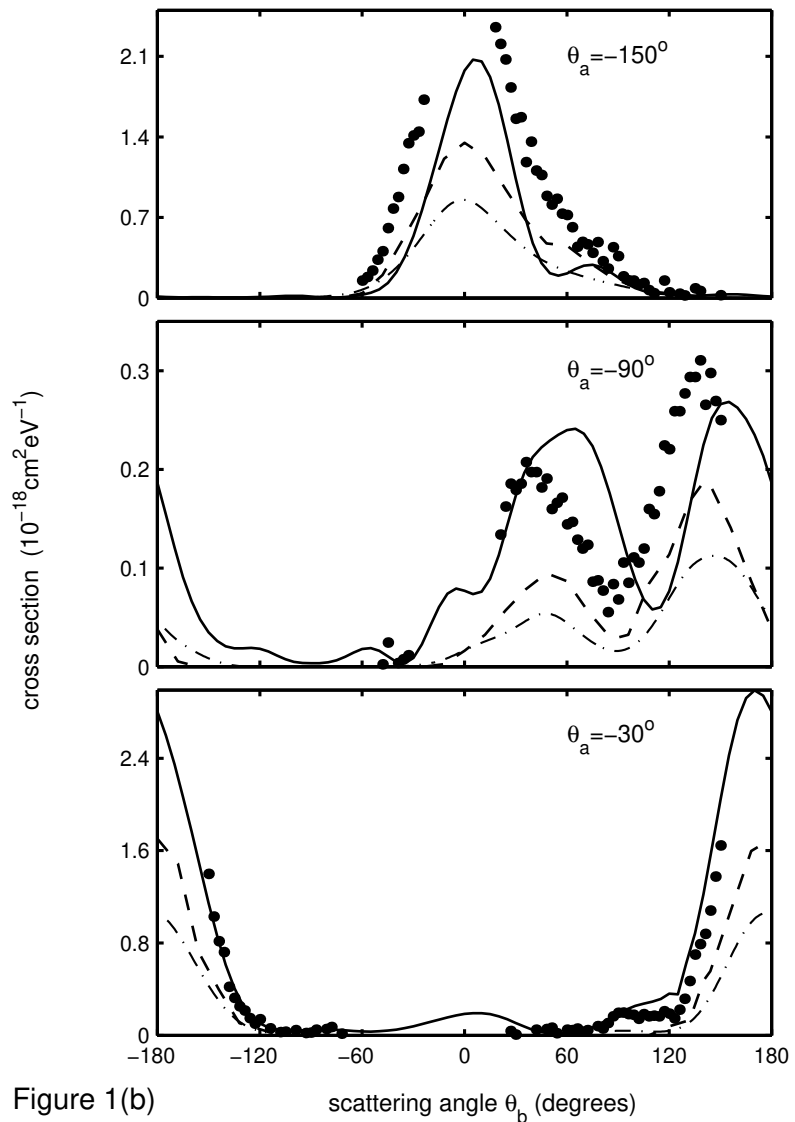


Figure 1(b)

scattering angle θ_b (degrees)

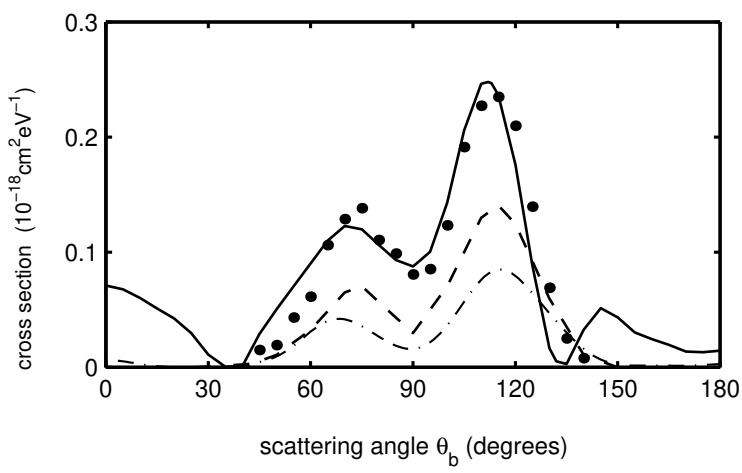


Figure 1(c)

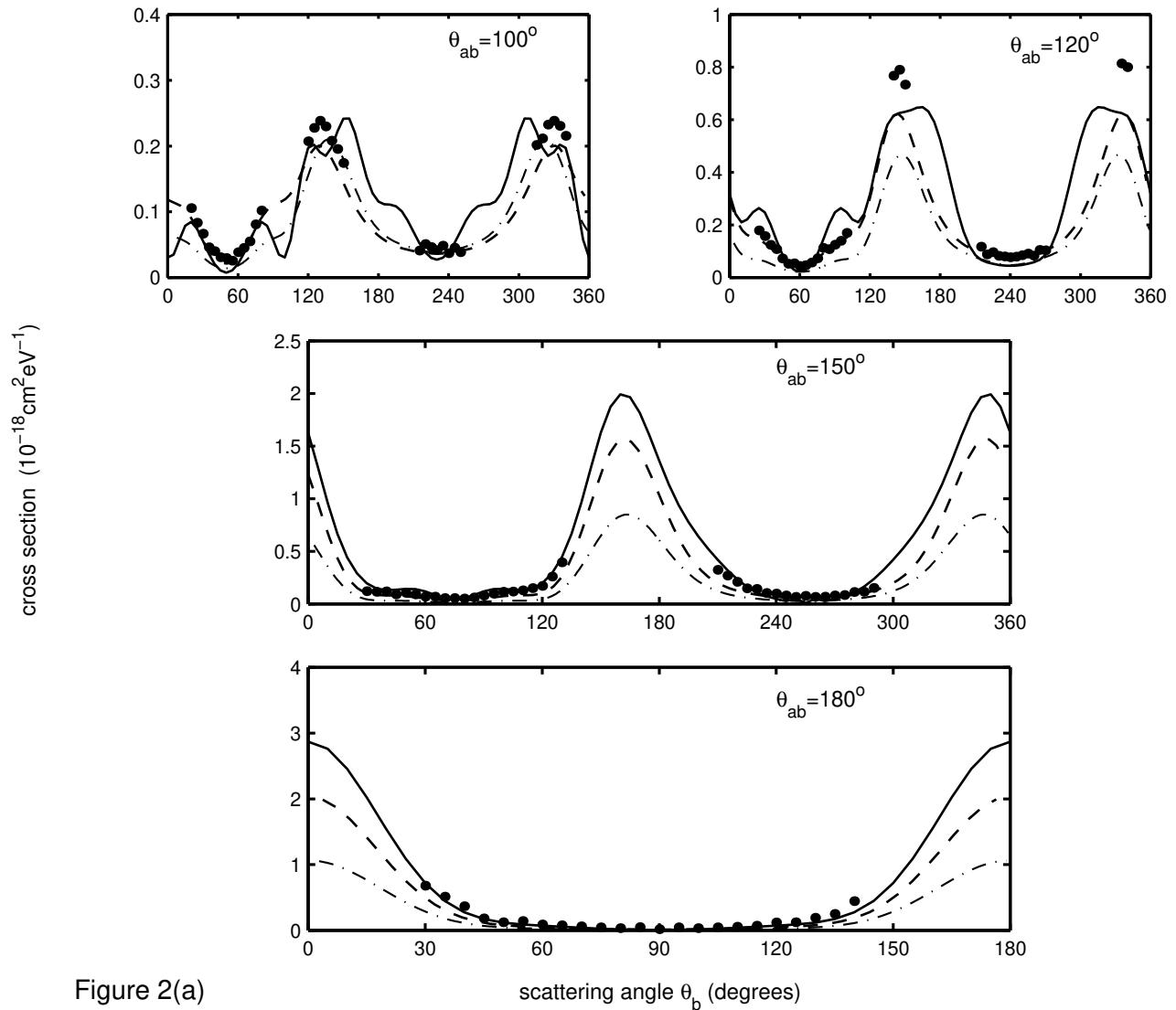


Figure 2(a)

scattering angle θ_b (degrees)

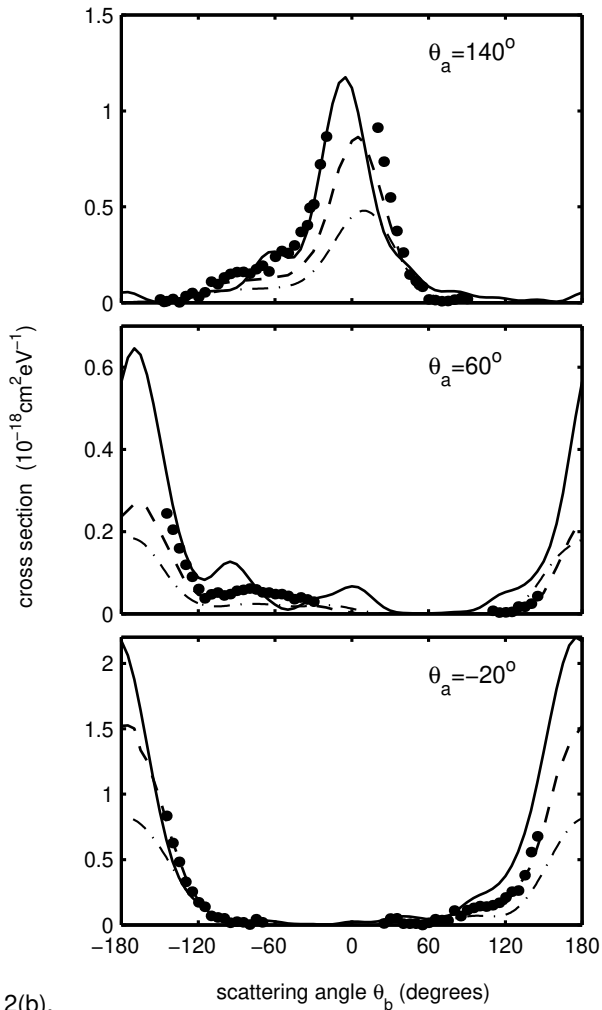


Figure 2(b).

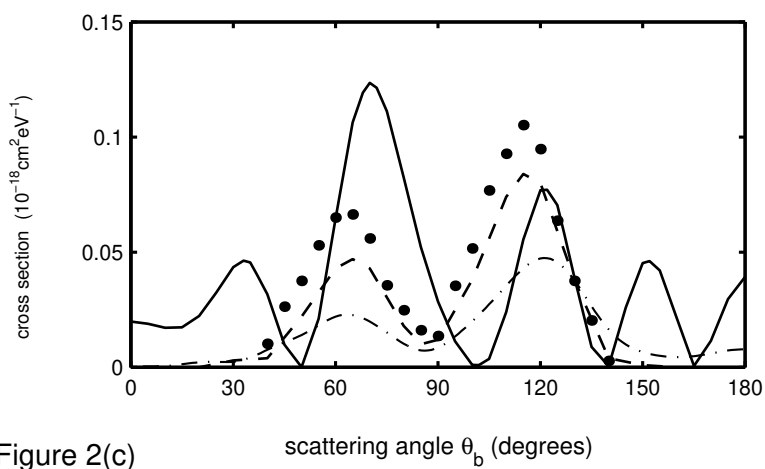


Figure 2(c)

scattering angle θ_b (degrees)

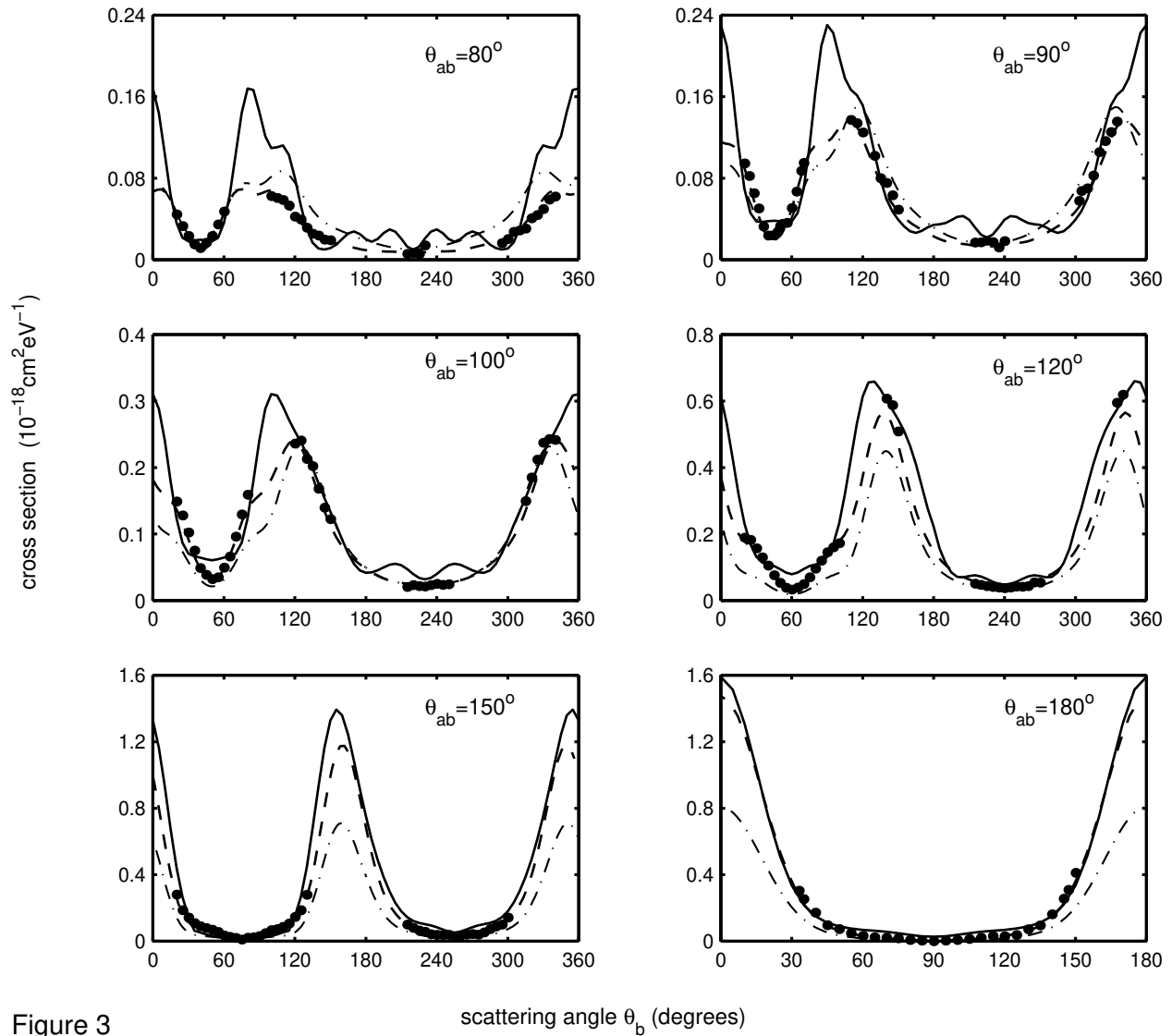


Figure 3

scattering angle θ_b (degrees)

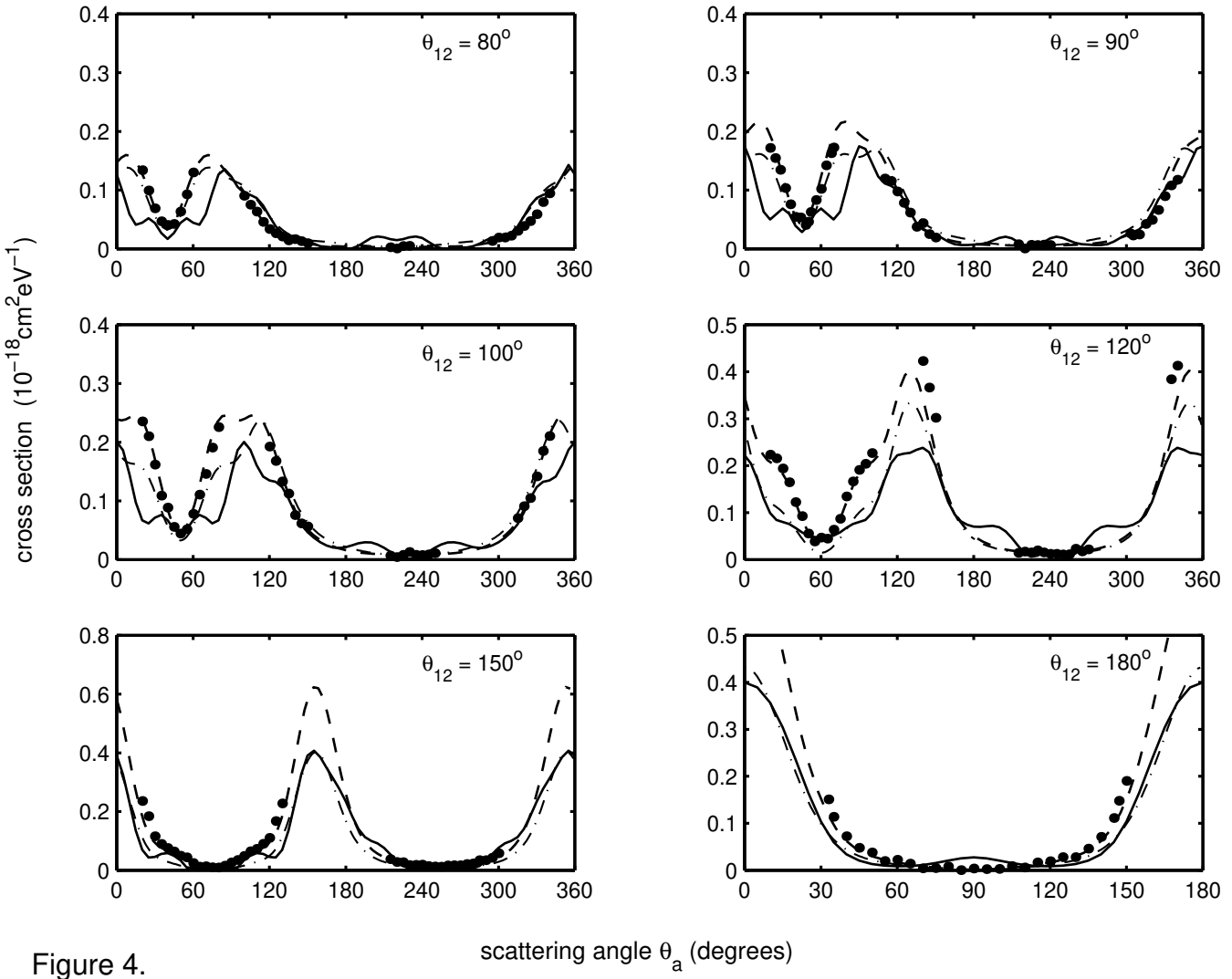


Figure 4.

scattering angle θ_a (degrees)

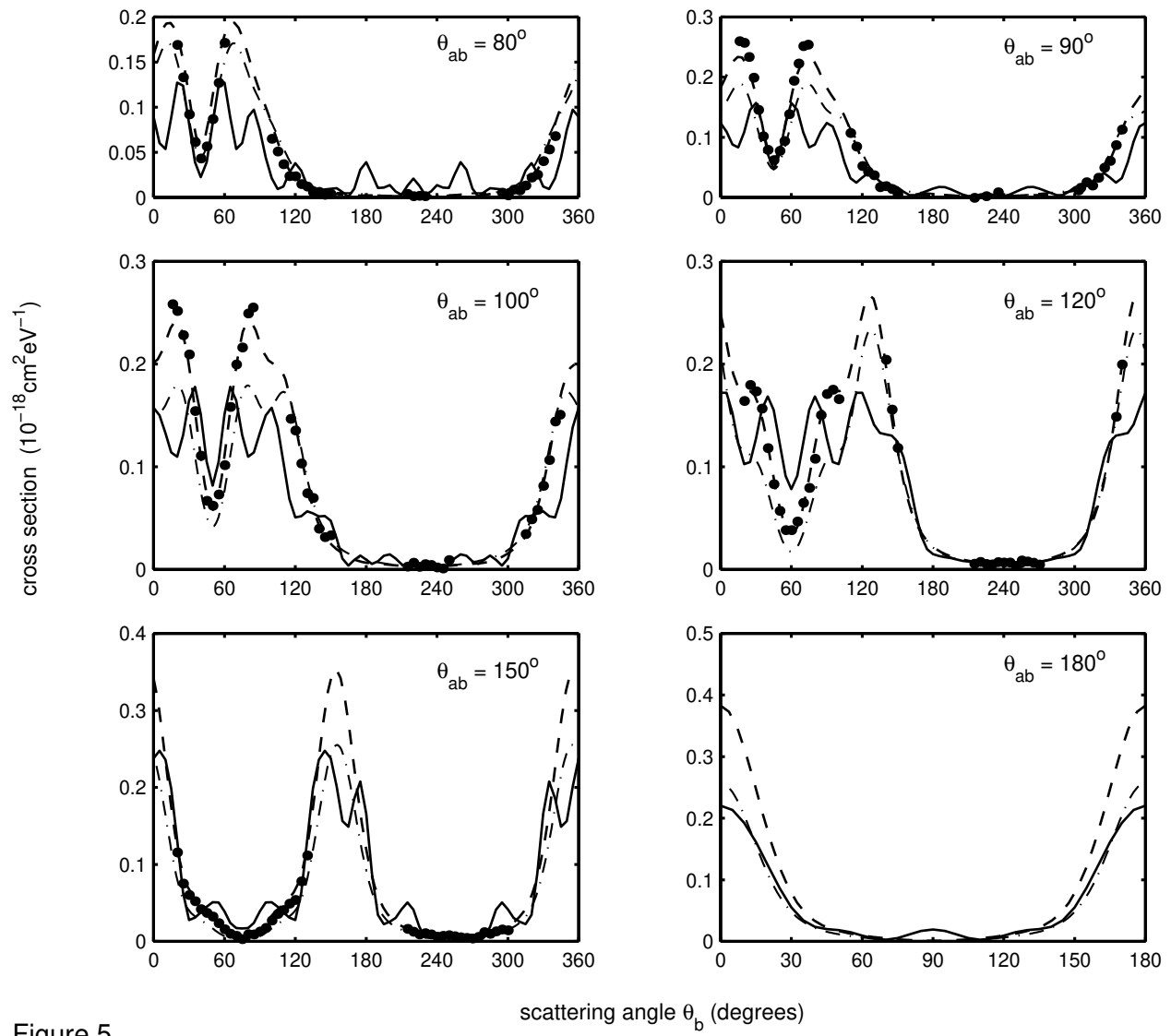


Figure 5